Journal of Magnetism and Magnetic Materials 449 (2018) 304–307

Contents lists available at ScienceDirect

Journal of Magnetism and Magnetic Materials

journal homepage: www.elsevier.com/locate/jmmm

Research articles

Magnetocaloric effect study of $Pr_{0.67}Ca_{0.33}MnO_3$-$La_{0.67}Sr_{0.33}MnO_3$ nanocomposite

Kalipada Das [a,*], R. Roy Chowdhury [b], S. Midda [a], Pintu Sen [c], I. Das [b]

[a] Department of Physics, Seth Anandram Jaipuria College, 10 Raja Naba Krishna Street, Kolkata 700005, India
[b] CMP Division, Saha Institute of Nuclear Physics, 1/AF, Bidhannagar, Kolkata 700064, India
[c] Variable Energy Cyclotron Centre, HBNI, 1/AF, Bidhannagar, Kolkata 700064, India

ARTICLE INFO

Article history:
Received 28 July 2017
Received in revised form 10 September 2017
Accepted 18 October 2017
Available online 19 October 2017

ABSTRACT

The present study involves investigaton of magnetocaloric effect of $Pr_{0.67}Ca_{0.33}MnO_3$-$La_{0.67}Sr_{0.33}MnO_3$ nanocomposite materials above room temperature. From application point of view in magnetic refrigeration our study highlights the enhancement of operating temperature region compared to the well known $La_{0.67}Sr_{0.33}MnO_3$ refrigerant material above room temperature. Comparison has also been made with the magnetocaloric properties of $La_{0.67}Sr_{0.33}MnO_3$ nanomaterials. The modification of the magnetocaloric entropy changes (broadening of the temperature dependent magnetic entropy change) is addressed due to the effect of the gradual melting of antiferromagnetic charge ordered state of the $Pr_{0.67}Ca_{0.33}MnO_3$ nanoparticles in such nanocomposite materials.

1. Introduction

In a drive to fight the adverse effect of global warming, researchers have put in enormous efforts to establish refrigeration techniques free of hazardous gases like the chloroflurocarbon (CFC) and hydrochlorofluorocarbon (HCFC). In case of magnetic refrigeration use of such harmful gasses can be controlled and also cooling efficiency is comparatively large compared to the gas compression cooling technology. For magnetic refrigeration, magnetocaloric effect (MCE) study is one of the most active field of research till date. MCE is the adiabatic temperature change (ΔT_{ad}) or isothermal magnetic entropy change (ΔS) of a magnetic material in presence of external magnetic field. Also in commercial purposes, relative cooling power (RCP) of a material plays an important role. RCP is the product of the maximum changes of the magnetic entropy and full width of the half maxima (FWHM) of its ($\Delta S(T)$) temperature span. There are numerous reports on MCE study in different kinds of materials namely intermetallic, oxides *etc.* which were published in previous few decades [1–18]. Though the magnetocaloric responses in intermetallic systems are significantly large compared to the oxide materials, but due to the high chemical stability, comparatively cheaper costing, insulating nature, these compounds are of utmost importance for studying magnetocaloric effect [7–9,14,17,19]. Another, attractive feature of the oxide materials specially in case of doped perovskite manganite materials (describe in the latter part) is that the ordering temperature (Currie temperature, T_C or Neel temperature, T_N) is large. In some materials the ordering temperature is even above the room temperature. Searching such good refrigerant magnetic materials is very important for employing in room temperature or high temperature applications.

The doped perovskite manganites, generally represented by $R_{1-x}B_xMnO_3$, where R is the trivalent rare-earth element (La, Pr, Gd, Dy *etc.*) and B is the bivalent element (Ca, Sr, Ba *etc.*). Among the doped perovskite manganites $La_{1-x}Sr_xMnO_3$ and $Pr_{1-x}Ca_xMnO_3$ are the most well studied materials as they exhibit interesting properties. Special attention had been paid to study the magnetoresistive and magnetocaloric effect study of the $La_{0.67}Sr_{0.33}MnO_3$ compounds due to its para-ferromagnetic transition which usually occurs above room temperature ($T \sim 360$ K) and its half metallic nature [20]. On the other hand $Pr_{0.67}Ca_{0.33}MnO_3$ compounds, exhibits charge ordered antiferromagnetic nature with decreasing temperature [20]. Since MCE is directly related to the suppression of the spin (magnetic) disorder, so usually maximum change of the magnetic entropy change appears at the vicinity of the transition temperature (para to ferromagnetic). To tune the ordering temperature of $La_{0.7}Sr_{0.3}MnO_3$ compounds, many attempts have been made namely the reduction of the particle size, substitution of La-site with different elements *etc.* [16,21]. By the reduction of the average particle sizes of the $La_{0.7}Sr_{0.3}MnO_3$ sample, the broadening of the peak in $-\Delta S(T)$ appears but the magnitude of MCE decreases. However, for $Pr_{0.7}Ca_{0.3}MnO_3$ compound, the physical properties are drastically modified with the application of the external magnetic field as well

* Corresponding author.
E-mail address: kalipadadasphysics@gmail.com (K. Das).

https://doi.org/10.1016/j.jmmm.2017.10.063
0304-8853/

as with the reduction of the particle size [21]. It may be emphasized that extra grain boundaries disorderness influence the magnetocaloric responses of the materials.

Main aim of this present study is that to investigate the MCE of the nanocomposite materials where $Pr_{0.67}Ca_{0.33}MnO_3$ nanoparticles (PCMO) are wrapped by the half metallic $La_{0.67}Sr_{0.33}MnO_3$ matrix. Moreover, the influence of grain boundaries of PCMO on MCE properties of LSMO have also been addressed.

We have synthesized the $Pr_{0.67}Ca_{0.33}MnO_3 - La_{0.67}Sr_{0.33}MnO_3$ nanocomposite material and studied the magnetocaloric effect of this nanocomposite material. In addition to that we have compared the magnetocaloric effect with its parent compound $La_{0.67}Sr_{0.33}MnO_3$ nanoparicles (LSMO) having average particle size ~ 20 nm. Our experimental results reveal that due to the introduction of the PCMO nanoparticles into the LSMO matrix, in addition to the shifting of the transition temperature (Currie temperature, $T_C = 335$ K) towards the room temperature, broadening of $-\Delta S(T)$ appears compared to the LSMO nanoparticles.

2. Sample preparation, characterizations and measurements

The preparation of the samples involved preparation of the PCMO nanoparticles by the following method. Preheated Pr_6O_{11}, $CaCO_3$ and MnO_2 were used having purity greater than 99.9 % as starting elements. The oxide materials (Pr_6O_{11} and $CaCO_3$) were converted to their nitrates form by using HNO_3 and dissolving them into millipore water. For dissolving MnO_2, appropriate amount of oxalic acid was mixed with nitric acid and finally dissolved into millipore water. All the above mentioned clear solutions were mixed up homogeneously in a beaker and suitable amount of citric acid was added. Extra water was evaporated slowly by using a water bath at T = 80–90 °C until the gel was formed. After gel formation, it was decomposed at slightly higher temperature (T = 200 °C) which resulted in a black porous powder was formed. In order to obtain crystalline PCMO nanoparticles, powder was annealed at 950 °C for 4 h.

By following similar procedure LSMO nanoparticles were prepared using La_2O_3, $Sr(NO_3)_2$ and MnO_2 (having average particle size ~ 20 nm) as the starting elements. However, for preparation of the nanocomposite $Pr_{0.67}Ca_{0.33}MnO_3$-$La_{0.67}Sr_{0.33}MnO_3$ materials, first, the PCMO nanoparticles (having average particle size ~ 46 nm) was prepared (described above). After the preparation of single phase PCMO nanoparticles, the amount of the LSMO gel was estimated and prepared such that the shell thickness should be ~ 10 nm. It is worth mentioning that the weight ratio of LSMO and PCMO in nanocomposite material is 2:1. PCMO nanoparticles were poured into the LSMO gel at the last stage and was stirred using a magnetic stirrer. By decomposing the gel at a slightly higher temperature (~ 200 °C), the black porous powder was formed which was pelletized and annealed at 900 °C for 4 h.

For characterization, room temperature X-ray diffraction study was employed using a Rigaku TTRAX-III diffractometer for powder form of nanocomposite and LSMO nanoparticles. Nanocomposite materials were also characterized by detailed study of high resolution transmission electron microscopy (HRTEM).

Magnetization and magnetocaloric properties measurements of the nanocomposite and LSMO nanomaterials, have been carried out using both physical properties measurement system (PPMS) and superconducting quantum interference device (SQUID) (Quantum Design).

3. Results and discussion

Room temperature X-ray diffraction patterns of LSMO nanoparticles and nanocomposite materials are shown in Fig. 1(a) and (b) respectively. Profile fittings were carried out by using $R\bar{3}C$ space group symmetry for LSMO nanoparticles. Whereas for nanocomposite materials, we have performed mixed phase analysis considering $R\bar{3}C$ and *pnma* (for PCMO counterpart) space groups. The profile fittings indicate about the single phase nature of the LSMO nanoparticles. No additional phases were observed in the nanocomposite materials except for LSMO and PCMO. For further characterization we have performed HRTEM studies for nanocomposite materials and the results are given in Ref. [22] in detail.

Before studying the magnetocaloric effect of any magnetic materials, the understanding about the nature of magnetic ground state is very important. Magnetization as a function of temperature at a fixed magnetic field is one of the general experiments from which many important informations can be understood, especially for the determination of the region involving its disorder-to order state transition. In our present study we have recorded temperature dependence of magnetization for nano composite materials in two different protocols: zero field cooled (ZFC) and field cooled (FC). In ZFC protocol, the sample was cooled down from its paramagnetic region (T = 380 K) in the absence of any external magnetic field. After reaching low temperature (T = 5 K) magnetization data was recorded during the warming cycle from 5–380 K in the presence of magnetic field. On the other hand in FC protocol the sample was cooled down to low temperature (T = 5 K) in the presence of the fixed magnetic field and then the data recorded during warming cycle (5–380 K) in the presence of same field (cooling field). For the nanocomposite material magnetization as a function of temperature is shown in Fig. 2 for different magnetic field. The experimental results indicate the predominant ferromagnetic like ground state of the material at the low temperature. Moreover, the paramagnetic to ferromagnetic transition temperature is observed to approach room temperature (300 K). In this context another worth mentioning point is the irreversibility between the ZFC and FC magnetization (bifurcation) which almost disappears in H $\geqslant$ 5 kOe external magnetic field. Such behavior indicate that whatever the cause of this bifurcation (spin disorder, pinning

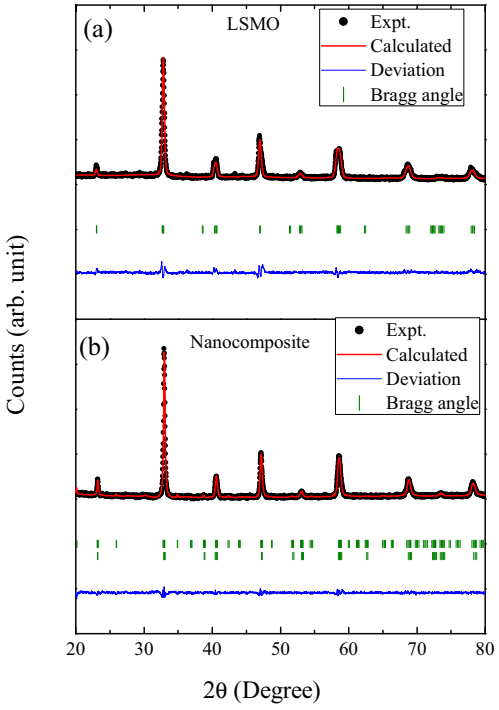

Fig. 1. Room temperature X-ray diffraction patterns along with profile fitting of (a) LSMO nanoparticles and (b) PCMO-LSMO nanocomposite material.

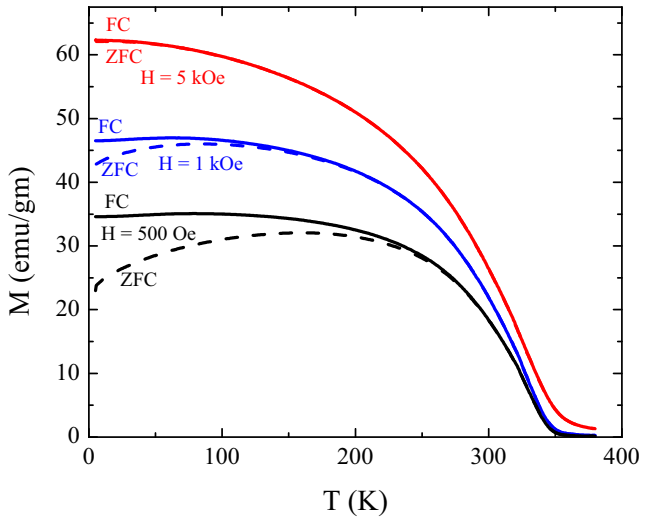

Fig. 2. Magnetization (M) as a function of temperature (T) for different external magnetic field (H) measured in zero field cooled (represents by dashed lines) and field cooled (represents by solid lines) protocols.

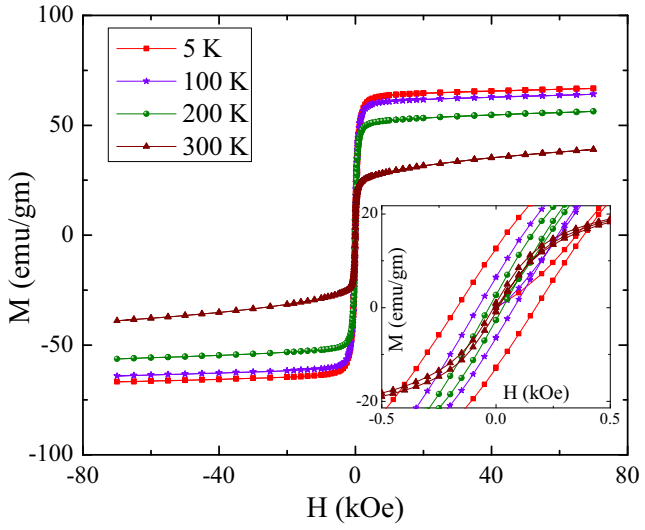

Fig. 3. Magnetization as a function of external magnetic field at different temperatures. Inset indicate the enlarged view at the low field region.

center, defects *etc.*), its effect is very small in case of the present nanocomposite material.

As mentioned earlier, the predominant ferromagnetic interaction at low temperature is also reflected in our magnetic isotherms measurement. The hysteresis loops of the nano composite sample were recorded at different temperatures, viz. at T = 5 K, 100 K, 200 K and 300 K. It is worth mentioning that, before recording the magnetization as a function of magnetic field at a fixed temperature, the sample was cooled down from its paramagnetic state (T = 380 K) in the absence of any external magnetic field to remove the effect of any previous measurement if present. Field dependent magnetization is shown in Fig. 3. This measurement indicate soft ferromagnetic nature of the material (magnetization almost saturated at lower value of the external magnetic field). At very low values of the magnetic field the hysteresis loop was present which can be observed in the inset of Fig. 3. In the low temperature region though significant irreversibility (coercive field $H_C = 250$ Oe for 5 K) was present, but at the vicinity of the room temperature ($T \geqslant 300$ K), the hysteresis effect is negligible.

From the temperature dependent and field dependent magnetization studies it is clear that the disorder to order transition is near to the room temperature and at T = 300 K (room temperature) almost reversible behavior of magnetization (no hysteresis nature) was observed. The previous observations and discussions led us to carry out study of the magnetocaloric effect of the nanocomposite material. Furthermore, inorder to compare the magnetocaloric responses of that nanocomposite material with LSMO nanoparticles, MCE study of the LSMO nanoparticles were also carried out.

Magnetocaloric entropy changes (ΔS) was determined from the magnetic isotherms data using Maxwell's thermodynamic relation, given by,

$$\Delta S = \int_0^H (\partial M/\partial T) dH \tag{1}$$

The calculated values of $-\Delta S$ as a function of temperature in the presence of different external magnetic field is given in Fig. 4(A). The numerical value of entropy changes ($-\Delta S$) is not very large in our present study but the ordering temperature (where maximum change of entropy appears) is very close to room temperature (a few Kelvin above). Fig. 4(A) exhibits significant broadening of the peak, which motivated us to calculate another important parameter, relative cooling power (RCP) of that material. RCP is generally estimated by the expression

$$RCP = \Delta S_{max} \times \Delta T_{FWHM} \tag{2}$$

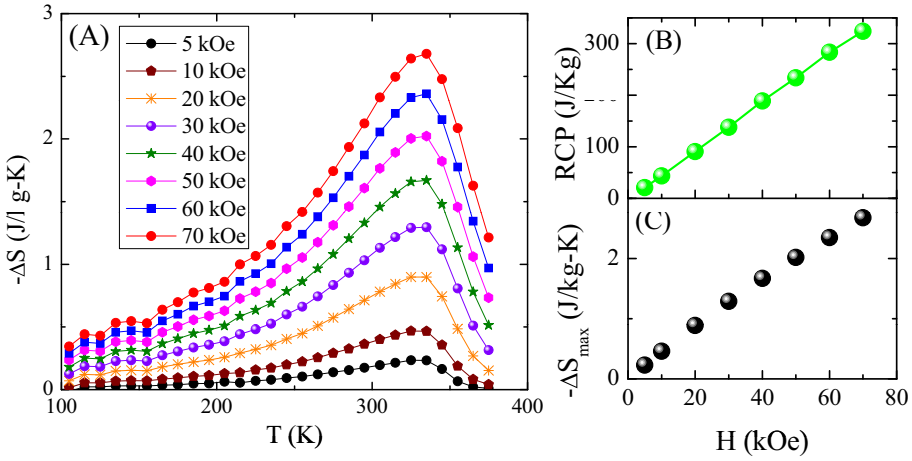

Fig. 4. (A) Magnetocaloric entropy changes as a function of temperature for different external magnetic field of the nanocomposite material. (B) and (C) represents the field dependent RCP and $-\Delta S_{max}$ respectively.

Table 1
Comparison of $-\Delta S$ and RCP of several *La-Sr-MnO₃* compounds with nanocomposite material.

Compound	Magnetic field (kOe)	$-\Delta S$	RCP (J/kg)	Ref.
$La_{0.75}Sr_{0.25}MnO_3$	15	1.50	65	[17]
$La_{0.65}Sr_{0.35}MnO_3$	10	2.12	106	[17]
$La_{0.67}Sr_{0.33}MnO_3$	50	1.69	211	[17]
$La_{0.67}Sr_{0.33}MnO_3$ (nano)	50	2.03	204	Present study
PCMO-LSMO nanocomposite	50	2.02	234	Present study

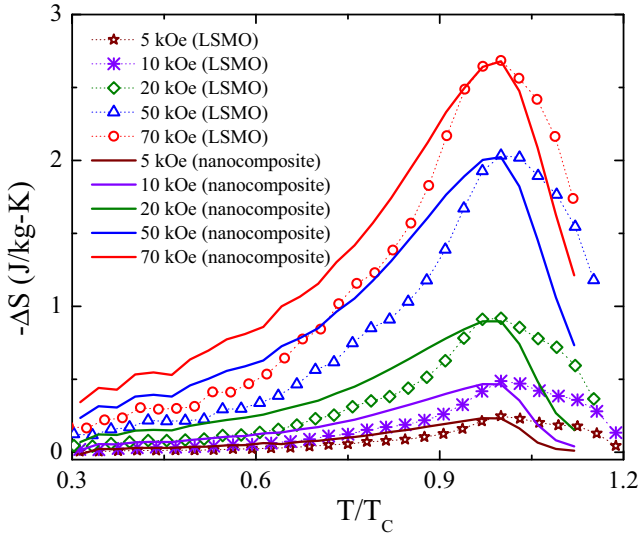

Fig. 5. (A) Magnetocaloric entropy changes as a function of normalized temperature (T/T_C) for different external magnetic field of the nanocomposite material and LSMO nanoparticles.

$-\Delta S_{max}$ is the maximum value of the change of the entropy (peak value) and ΔT_{FWHM} is the full width at half maxima in temperature scale. The estimated RCP as function of magnetic field is given in Fig. 4(B) which indicates that the RCP value is significantly large. Moreover, the variation of the $-\Delta S_{max}$ as a function of magnetic field also shown in Fig. 4(C). The magnetocaloric entropy change and RCP of several La-Sr-MnO_3 compounds with the nanocomposite materials are compared in Table 1.

Now to compare the magnetocaloric properties of the nanocomposite and LSMO nanoparticles, we have calculated $-\Delta S$ as a function of temperature for LSMO up to 380 K (measurement limit). Since in case of LSMO nanoparticles the ordering temperature (T_C) is larger compared to nano composite materials it was not possible to calculate RCP from the experimental data of LSMO nanoparticles.

In Fig. 5 we have compared $-\Delta S$ as a function of (T/T_C) to get a clear view of the enhancement of the broadening of the nanocomposite material compared to LSMO. Interestingly our study indicates that ΔS_{max} is almost same for nanocomposite and LSMO nanoparticles. However, in case of nanocomposite materials, the broadening of temperature (below T/T_C region towards room temperature) is significantly large compared to its parent compound LSMO nanoparticles which indicate good refrigerant quality of this nanocomposite material.

4. Conclusions

To summarize, we have synthesized $Pr_{0.67}Ca_{0.33}MnO_3$ – $La_{0.67}Sr_{0.33}MnO_3$ nanocomposite and $La_{0.67}Sr_{0.33}MnO_3$ nanoparticles by sol–gel method. Investigations of the magnetocaloric properties indicate the relative cooling power of nanocomposite material to be significantly large near room temperature. In addition to that the numerical peak values of $-\Delta S$ (magnetocaloric entropy change) is observed to be almost similar for two materials (nanocomposite and LSMO nanoparticles). Moreover the peak of $-\Delta S(T)$ is shifted towards the room temperature and its broadening is enhanced for nanocomposite material which may be important for technological point of view.

Acknowledgements

The work was supported by Department of Atomic Energy (DAE), Govt. of India.

References

[1] A.M. Tishin, Y.I. Spichkin, The Magnetocaloric Effect and its Applications, Institute of Physics Publishing, Bristol and Philadelphia, 2003.
[2] K.A. Gschneidner Jr., V.K. Pecharsky, A.O. Tsokol, Rep. Prog. Phys. 68 (2005) 1479–1539.
[3] A.O. Pecharsky, K.A. Gschneidner Jr., V.K. Pecharsky, J. Appl. Phys. 93 (2003) 4722–4728.
[4] O. Tegus, E. Bruck, K.H.J. Buschow, F.R. deBoer, Nature 415 (2002) 150–152.
[5] H. Wada, Y. Tanabe, Appl. Phys. Lett. 79 (2001) 3302–3304.
[6] H. Wada, Y. Tanabe, M. Shiga, H. Sugawara, H. Sato, J. Alloys Compd. 316 (2001) 245–249.
[7] N.S. Bingham, P. Lampen, M.H. Phan, T.D. Hoang, H.D. Chinh, C.L. Zhang, S.W. Cheong, H. Srikanth, Phys. rev. B 86 (2012) 064420.
[8] P. Lampen, A. Puri, M.H. Phan, H. Srikanth, J. Alloys Compd. 512 (2012) 94–99.
[9] P. Lampen, N.S. Bingham, M.H. Phan, H. Kim, M. Osofsky, A. Pique, T.L. Phan, S. C. Yu, H. Srikanth, Appl. Phys. Lett. 102 (2013) 062414.
[10] M.H. Phan, S. Chandra, N.S. Bingham, H. Srikanth, C.L. Zhang, S.W. Cheong, T.D. Hoang, H.D. Chinh, Appl. Phys. Lett. 97 (2010) 242506.
[11] N.K. Singh, K.G. Suresh, A.K. Nigam, S.K. Malik, J. Appl. Phys. 97 (2005) 10A301.
[12] T. Samanta, I. Das, S. Banerjee, Appl. Phys. Lett. 91 (2007) 152506.
[13] T. Samanta, I. Das, S. Banerjee, Appl. Phys. Lett. 91 (2007) 082511.
[14] K. Das, T. Paramanik, I. Das, J. Magn. Magn. Matter. 374 (2015) 707–710.
[15] K. Das, S. Banik, I. Das, Mater. Res. Bull. 73 (2016) 256–260.
[16] T. Samanta et al., Phys. Rev. B 91 (2015) 020401(R).
[17] M.H. Phan, S.C. Yu, J. Magn. Magn. Mater. 308 (2007) 325.
[18] A. Biswas, S. Chandra, M.H. Phan, H. Srikanth, J. Alloys Comp. 545 (2012) 157.
[19] P. Lampen, N.S. Bingham, M.H. Phan, H. Srikanth, H.T. Yi, S.W. Cheong, Phys. Rev. B 89 (2014) 144414.
[20] S.W. Cheong, H.Y. Hwang, in: Y. Tokura (Ed.), Contribution to Colossal Magnetoresistance Oxides, Monographs in Condensed Matter Science, Gordon and Breach, London, 1999.
[21] Y.F. Wang, H. Yang, J. Supercond. Nov. Magn. 8 (2013) 2190, https://doi.org/10.1007/s10948-013-2190-8.
[22] K. Das, B. Satpati, I. Das, RSC Adv. 5 (2015) 27338.